Analyst

Accepted Manuscript

This article can be cited before page numbers have been issued, to do this please use: S. Benítez-Martínez, E. Caballero-Díaz and M. Valcarcel, *Analyst*, 2016, DOI: 10.1039/C6AN00357E.

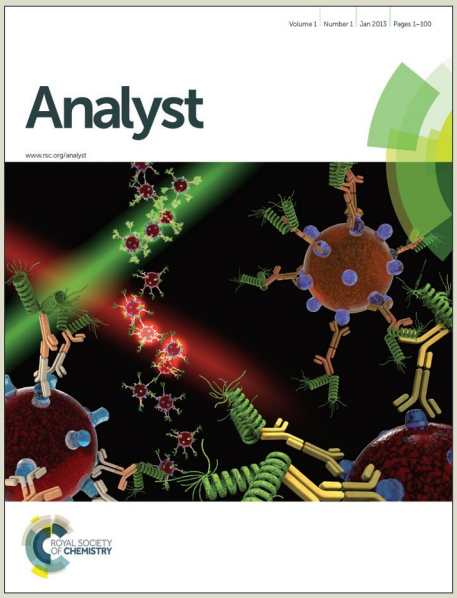

ROYAL SOCIETY OF CHEMISTRY

www.rsc.org/analyst

View Article Online
DOI: 10.1039/C6AN00357E

Development of a biosensing system for tacrine based on nitrogen-doped graphene quantum dots and acetylcholinesterase

S. Benítez-Martínez[*], E. Caballero-Díaz[*], M. Valcárcel[#]

Department of Analytical Chemistry, University of Córdoba, E-14071 Córdoba, Spain
Phone/Fax +34 957 218616;E-mail: qa1meobj@uco.es

Abstract

This work presents a novel fluorescent sensor for determination of tacrine by combining the magnificent fluorescence properties of nitrogen-doped graphene quantum dots (N-GQDs) with the high potential of acetylcholinesterase (AChE) enzyme for screening its inhibitors. Tacrine was the first drug approved for Alzheimer´s disease and it is currently used in several therapeutic treatments given its activity as reversible inhibitor of AChE. The principle of the developed biosensor relies on the fact that the native fluorescence of the synthesized N-GQDs is quenched by interaction with enzymatic reaction products, and the inclusion of tacrine in assay solution results in the gradual recovery of the original fluorescence in an inhibitor concentration-dependent manner. While N-GQD fluorescence was not directly affected by tacrine, the inclusion of an AChE based-enzymatic system allowed for its determination with a detection limit (S/N=3) of 1.22 µM. This biosensor was demonstrated to be simple, rapid and reproducible (%RSD 4.87, n=7) for analysis of tacrine in aqueous solutions.

Keywords: graphene quantum dots, nitrogen doped, acetylcholinesterase, tacrine, inhibitor, Alzheimer`s disease, fluorescent, biosensor.

[#]**Corresponding author.** Tel./Fax: +34 957 218616; E-mail: qa1vacam@uco.es

[*]Both authors contributed equally to this work.

View Article Online
DOI: 10.1039/C6AN00357E

1. Introduction

Carbon based nanoparticles (CNPs) have been widely used in the Analytical Chemistry field, resulting to be extremely useful tools in all the stages involved in the analytical procedure (i.e. sample treatment, separation and detection). In this context, CNPs have allowed for developing new analytical methodologies and improving other well-established analytical processes. Within the detection step, CNPs have been widely devoted to the fabrication of electrochemical and optical (bio)sensors taking advantage of their exceptional properties, such as large specific area and ability to promote electron and/or charge transfer in electrochemical interactions. Multiplexed sensing and imaging strategies that enable detection of several analytes in parallel by using different nanoparticles and readout systems at the same time, have been recently reviewed.[1] CNPs might be modified with other materials, such as metal nanoparticles, proteins and aptamers, among others, in order to improve their reactivity and obtain better selectivity and sensibility.[2] Most recently, fluorescent CNPs, namely, graphene quantum dots (GQDs), have attracted much attention in optical (bio)sensing applications thanks to their fluorescence activity, robust chemical inertness, excellent photostability, high biocompatibility, tunable fluorescence emission, high solubility and ease of synthesis by using a wide range of methodologies and different carbon sources.[3] These outstanding properties justify the great number of scientific publications involving the use of GQDs as sensing platforms for determination of metallic ions,[4,5] small organic molecules or biomaterials.[6-8] In order to improve their reactivity and fluorescence quantum yield, the structure of GQDs have been modified by incorporating other atoms in the hexagonal carbon honeycomb lattice such as nitrogen,[9] sulfur,[10] and both of them.[11]

Recent advances in sensing techniques have revealed the potential use of biomolecules as recognition elements, such as enzymes, antibodies and aptamers. Although the

View Article Online
DOI: 10.1039/C6AN00357E

development of sensors by integration of these biomolecules with nanomaterials as transducing elements is a challenging issue, their conjunction might lead to better results of sensitivity and selectivity in the sensing devices.[12] In line with this proposal, acetylcholinesterase (AChE) is one of the most employed enzymes. This enzyme is present in the neuromuscular junctions and is the responsible for the hydrolysis of the neurotransmitter acetylcholine into choline and acetate.[13] In some neurodegenerative disorders, like myasthenia gravis, senile dementia, Alzheimer and Parkinson diseases, inhibition of AChE is a fundamental therapeutic step.[14] Interestingly, several sensing applications based on the use of AChE have been developed over the last decade taking advantage of nanostructures, such as silver,[15] silica,[16] and gold nanoparticles,[17] carbon nanotubes[18] and most recently, graphene[19] and graphene oxide,[20] for the detection and quantification of different compounds, principally pesticides.

Herein, we develop a novel fluorescent sensor based on the combination of nitrogen-doped GQDs (N-GQDs) and AChE for the determination of tacrine, a drug currently used to treat patients with Alzheimer's disease that acts as cholinesterase inhibitor. It is believed that low levels of chemical messenger acetylcholine in the brain are responsible for some Alzheimer's disease symptoms. Thus, cholinesterase inhibitors are used in therapeutic treatments to block the AChE activity, and thus, to slow the hydrolysis of acetylcholine and compensate its low levels.[21] The methodology presented in this communication is a simple and very sensitive sensing approach involving the use of N-GQDs as fluorescent probes and an AChE-based system as biorecognition element for analysis of tacrine in aqueous samples.

2. Materials and methods

2.1. Reagents and standards

View Article Online
DOI: 10.1039/C6AN00357E

All chemical reagents were of analytical grade and used as received without further purification. Citric acid (≥ 99.0 %), used as carbon source in the GQDs synthesis procedure, and ammonia (≥ 25%), used as nitrogen source in the doping of GQDs, acetylcholinesterase (AChE) from *Electrophorus electricus* (200-1000 $U \cdot mg^{-1}$ protein), acetylthiocholine chloride (ATC) (≥ 99.0 %) and tacrine (1,2,3,4,-tetrahydroacridin-9-amine) (≥ 99.0 %), were all purchased from Sigma-Aldrich (Madrid, Spain).

For purifying the N-GQD synthesis solution, dialysis membranes (3500 Da cut off) were also acquired from Sigma–Aldrich (Madrid, Spain). Working solutions of N-GQDs were prepared and pH adjusted daily.

Formic acid (≥ 99%) was provided by Panreac Chemical, SAU (Barcelona, Spain). Ultra-pure water was obtained from a Milli–Q purification system (Millipore) (Madrid, Spain) with a resistivity of 18.2 MΩ/cm and used for preparation of all solutions.

AChE stock solutions (1 $mg \cdot mL^{-1}$) were prepared following the manufacturer´s instructions. Briefly, AChE was dissolved in 20 mM Tris buffer solution (pH 7.5) containing 1 $mg \cdot mL^{-1}$ of bovine serum albumin (BSA) in order to stabilize the enzyme. AChE solution was stored refrigerated in the dark at 4ºC until use. ATC stock solutions were prepared at a concentration of 10 $mg \cdot mL^{-1}$ in double-distilled water and stored at 4ºC. Aqueous solutions of tacrine were prepared at a concentration of 500 μM and stored at 4ºC in the dark.

2.2. Instrumentation

Fluorescence emission spectra were recorded on a PTI QuantaMaster™ spectrofluorimeter from Photon Technology International (Barcelona, Spain) equipped with a 75 W xenon short arc lamp and an 814 PTM detection system. The software

View Article Online
DOI: 10.1039/C6AN00357E

FeliX32 was used for data acquisition and instrument control. All measurements were made in quartz microcuvettes of 10 mm lightpath (Hellma Analytics).

Fourier transform mid infrared (FT-MIR) spectra were obtained on a Bruker Tensor 27FT-MIR spectrophotometer equipped with a Hyperion 2000 microscope, using KBr pellets.

High-resolution transmission electron microscopy (HRTEM) images were acquired with a JEOL JEM 2010 electron microscope available at the Research Support Service (SCAI) of the University of Córdoba (Córdoba, Spain). The instrument has a point-to-point resolution of 0.194 nm and operated at a medium acceleration voltage of 200 kV.

2.3. Synthesis of N-GQDs

N–GQDs were obtained by using citric acid and ammonia as carbon and nitrogen sources, respectively, following a hydrothermal synthesis procedure slightly modified with respect to that described by Tam et *al*.[9] To this end, 12 mL of 1 mg·mL^{-1} citric acid aqueous solution and 1.5 mL of 25% v/v ammonia were placed into a teflon-lined stainless steel autoclave reactor and heated in an oven for 3 h at 200ºC. The N-GQD solution obtained was adjusted to pH 9 with formic acid, dialyzed for 4 hours using a 3500 Da cut off membrane and stored at 4 ºC in an amber bottle. Undoped GQDs were synthesized according to the experimental protocol described in a previous work.[22]

2.4. Sensing method for tacrine determination

For the performance of the sensing method, 100 µL of AChE aqueous solution (1 mg mL^{-1}) were incubated with different amounts of tacrine for 15 min at 37ºC in the dark. After this time, 140 µL of a 10 mg·mL^{-1} ATC aqueous solution were added, mixed and incubated again at 37ºC for another 5 min. Finally, 500 µL of 25–fold diluted N–GQD

View Article Online
DOI: 10.1039/C6AN00357E

aqueous solution (pH 6) were added and left to stand for 5 min at room temperature in darkness before the fluorescence measurements. Fluorimetric analysis was directly performed in a 10 mm quartz microcuvette, setting an excitation wavelength of 355 nm and emission range between 380 and 600 nm (maximum peak at 440 nm).

The validation of our sensing strategy was finally performed by analysis of river water samples collected from Guadalquivir river (Córdoba, Spain). Samples were stored at 2-8ºC in the dark prior to use.

3. Results and discussion

3.1. Characterization of N–GQDs

Nitrogen-doped graphene quantum dots synthesized in this work were circular sheets with an average diameter of 4.6±0.78 nm, being characterized by HR-TEM.

Infrared study revealed the presence of namely hydroxyl and carboxyl functional groups which confer them excellent water solubility and great stability. The FT-IR spectrum of the doped GQDs reveals absorption peaks of the stretching vibration of C=O (at 1718 cm^{-1}) and the deformation of C–O (at 1392 cm^{-1}) in the carboxylic group. The stretching vibration of the H-bonded associated to –OH functional groups were assigned to the band around 3400 cm^{-1}. The band observed at 1200 cm^{-1} approximately, was attributed to de C–N stretching and that observed at 1500-1780 cm^{-1} corresponds to the C=O stretching of carboxylic groups. Finally, the band around 3400 cm^{-1} was assigned to the O–H stretching vibration of hydroxyl group with a possible contribution of the N–H. Figure 1 shows a HR-TEM image and a FT-IR spectra of the N-GQDs.

<<Figure 1>>

View Article Online
DOI: 10.1039/C6AN00357E

N-GQDs obtained were finally characterized by fluorescence spectroscopy. They were excitation wavelength independent, that is, the maximum fluorescence emission did not shift when these nanoparticles were excited at different wavelengths. N-GQDs exhibit their highest fluorescence emission at 440 nm when they were excited al 355 nm. The N-GQDs quantum yield was 42% using quinine sulphate as reference.

3.2 Principle of AChE-GQD biosensor

A general picture illustrating the principle of the proposed biosensor for determination of tacrine is shown in Figure 2. As can be observed, the inhibition potential of this drug is used for modulating the enzymatic activity of AChE what is finally assayed by changes in the native fluorescence of N-GQDs.

<<Figure 2>>

Tacrine is known to inhibit the AChE activity by reversible binding to both α- and peripheral anionic sites of enzyme.[23,24] Specifically in this work, AChE catalyzed the splitting of ATC into thiocholine and acetate, resulting in a reduction of native fluorescence of N-GQDs. This quenching effect might be ascribed to interaction mechanisms of N-GQDs with the hydrolysis reaction products (i.e. thiocholine and acetate). However, the introduction of tacrine into solution inhibited the enzymatic activity and allowed for recovery of the original fluorescence of N-GQDs in an inhibitor concentration-dependent manner. AChE was therefore used as biorecognition element

View Article Online
DOI: 10.1039/C6AN00357E

for sensitive detection of tacrine, while N-GQDs acted as fluorescent probes for enzyme inhibitor screening.

3.3 Optimization of AChE-GQD assay

Optimization studies were all performed in the absence of inhibitor, with the main purpose of maximizing the quenching effect produced by enzymatic reaction products on N-GQD fluorescence. The principal variables influencing the quenching effect were taken into account in these studies, namely: type of GQDs, AChE concentration, ATC concentration, ATC solution pH, GQD solution pH, GQD dilution, and several incubation times. Once optimum working conditions were defined, biosensor was assayed for determination of tacrine by measuring the inhibition efficiency as a function of inhibitor concentration.

3.3.1 Type of GQDs

With the aim of selecting the most appropriate nanoparticles for maximizing the response of fluorescent sensor, two different types of GQDs were firstly investigated: N-GQDs and undoped GQDs. The corresponding experimental protocols for synthesis of both nanoparticles were previously commented in section 2.3. In order to optimize the response of nanoparticles towards changes provoked by reaction products, parallel experiments were conducted under the same experimental conditions but using both types of GQDs. N-GQDs were found to generate a more stable and stronger fluorescence signal compared with undoped GQDs. While the maximum emission for undoped GQDs was recorded at 464 nm, N-GQDs showed its maximum fluorescence peak at 440 nm. Additionally, a greater quenching effect on the fluorescence of N-GQDs was observed when the enzymatic reaction took place, possibly due to the fact that these nanoparticles interacted to a greater extent with enzymatic hydrolysis

View Article Online
DOI: 10.1039/C6AN00357E

products than undoped GQDs. Findings from this study was determining in selecting N-GQDs for subsequent experiments. Figure 3 shows a typical fluorescence spectrum obtained from N-GQDs+ATC and N-GQDs+AChE+ATC. As can be appreciated, the inclusion of AChE in the system activated the enzymatic reaction and the resulting products caused a significant decrease in fluorescence of N-GQDs+ATC.

<<Figure 3>>

3.3.2 Effect of AChE concentration

The influence of the enzyme concentration was examined in order to get better reaction activity of AChE to produce thiocholine product. For this purpose, different AChE concentrations (0-27.4 $U \cdot mL^{-1}$) were tested while the rest of experimental conditions remained constant. The experimental protocol was as follows: firstly, different volumes of AChE stock solution (1 $mg \cdot mL^{-1}$) were incubated with aliquots of ATC stock solution (400 µL; 2 $mg \cdot mL^{-1}$) for 30 min at 37ºC in the dark. Next, 500 µL of an aqueous dilution of N-GQDs (1:10) were added to the mixture and incubated for 1 h more at room temperature in the dark. Figure 4 shows the effect of AChE concentration on quenching of fluorescence of N-GQDs. Results demonstrate that the decrease in fluorescence was associated with formation of thiocholine in the hydrolysis reaction of ATC, which was mediated by AChE. As can be seen, a higher quenching effect was observed by increasing the AChE concentration in the system. Finally, 27.4 $U \cdot mL^{-1}$ was chosen as optimum concentration of enzyme for subsequent experiments.

View Article Online
DOI: 10.1039/C6AN00357E

<<Figure 4>>

3.3.3 Study of concentration and pH of ATC solution

The impact of ATC amount on fluorescence quenching was next investigated by monitoring the decrease in fluorescent signal of N-GQDs as a function of substrate concentration. Results are shown in Fig. S1a and clearly indicated that along with the increasing substrate concentration, the decrease in N-GQD fluorescence was more significant. However, the curve became asymptotic over the concentration of 14.16 mM and consequently, this value was taken as optimal ATC concentration. Fig. S1b represents the effect of pH on the fluorescence quenching in the AChE-GQD system. As observed, no considerable differences were reported by using ATC aqueous solutions with varying pH in the range 6-9. Therefore, pH of ATC solution was dismissed as influential variable and substrate solutions were used without previous pH adjustment.

3.3.4 Influence of N-GQD solution pH

Numerous reports in literature have described the use of GQDs as fluorescent nanosensors sensitive to pH fluctuations, since their optical properties are highly dependent on the solution pH. In a recent work, our research group developed a fluorescent GQD-based sensor for determination of phenols in olive oils. The pH of aqueous solution of GQDs was found to be a critical parameter for the fluorescence intensity of nanoparticles.[25] In this same context, Shi et al. recently demonstrated an enhanced fluorescence intensity of oxygen-rich N-GQDs by increasing the solution pH in the range 3-8. Authors stated that the higher degree of deprotonation of nitrogen and

View Article Online
DOI: 10.1039/C6AN00357E

oxygen atoms on the surface of GQDs, as increasing the solution pH, changed the electron distributions and consequently, varied the fluorescence intensity.[26] In our study, a detailed investigation of the variation in quenching effect on the fluorescence of N-GQDs was carried out by modifying the pH value of aqueous dilution of N-GQDs from 5 to 10. As shown is Figure S2 the fluorescence attenuation was quite similar at pH 5 and 6, although it was slightly superior at pH 6. From this value on, quenching decreased gradually until reaching at minimum at pH 10. Consequently, pH 6 was chosen as optimal value for further studies.

3.3.5 Study of the N–GQD dilution

N-GQDs were obtained following the synthetic route described in section 2.3. The concentration of nanoparticles after dialysis were calculated to be 0.146 $mg \cdot mL^{-1}$. In order to obtain the maximal fluorescence attenuation to develop the sensing system, different dilutions of N-GQD solution obtained from dialysis were tested: 1:25, 1:10, 1:5, 1:2 and 1:1. For this study, 500 µL of each dilution of N-GQDs were mixed with 500 µL of the enzymatic system (100 µL of AChE and 400 µL of ATC). The enzyme and substrate concentrations used in this study were 27.4 $U \cdot mL^{-1}$ and 14.16 mM, respectively. The best results in terms of quenching were obtained when the enzymatic part was mixed with 500 µL of 1:25 GQD dilution (Figure 5). Increasing concentrations of N-GQDs caused a decrease in fluorescence quenching, probably due to the fact that the proximity between nanoparticles could limit the interaction with enzymatic reaction products (i.e. thiocholine and acetate). On the contrary, in more diluted solutions, nanoparticles were more detached from others and thus the interaction with the enzymatic reaction products were more efficient, resulting in a greater attenuation of fluorescence.

View Article Online
DOI: 10.1039/C6AN00357E

<<Figure 5>>

3.3.6 Study of AChE-ATC incubation time

Once the enzyme and substrate concentrations were fixed, the time needed by the enzyme to transform the substrate into products was studied. As it is well-known, there is a directly proportional relationship between incubation time and the generated products, i.e., the longer incubation time, the greater is the amount of product generated. For the development of this study, working solutions of N-GQDs, AChE and ATC were used at optimized conditions (1:25 dilution, 27.4 $U \cdot mL^{-1}$ and 14.16 mM, respectively). The temperature for incubation period was 37ºC in all cases. The tested incubation times were 3, 5, 10, 15, 20 and 30 min. As can be seen in Figure S3 a slightly greater quenching effect was achieved at 30 min. However, no notable differences were observed among all the incubation times investigated, and consequently, 5 min were selected as optimal incubation time between AChE and ATC, also reaching a compromise between rapidity and sensitivity of analysis.

3.3.7 Study of enzymatic system and N–GQD solution reaction time

The time of contact between the enzymatic reaction products and the N-GQD dilution was also optimized. In order to achieve an adequate interaction between them, leading to a maximized fluorescence quenching, eight different times were studied, namely: 5, 10, 20, 30, 40, 60, 75 and 90 min. As can be seen from Figure S4, differences in the obtained quenching for each studied time were not important, what was demonstrated by the almost indiscernible difference in quenching for times of 5 min (0.64) and 90

View Article Online
DOI: 10.1039/C6AN00357E

min (0.69). For this reason, an interaction time of 5 min between the enzymatic system and the doped nanoparticles was selected for further studies.

3.3.8 Study of AChE-tacrine incubation time

Tacrine, selected as target analyte in this work, acts as inhibitor of the AChE activity. Therefore, the transformation of ATC in thiocholine and acetate is blocked in the presence of this inhibitor. The time required to obtain a greater interaction between AChE and tacrine was also investigated. To this end, times of 5, 10, 20 and 30 min were studied. In a first step, AChE solution was incubated with tacrine at 37ºC for different times. Subsequently, ATC solution was added into solution and incubated at 37ºC for 5 min. Finally, N-GQD solution was added, mixed and left to stand for another 5 min before fluorimetric analysis. Figure S5 depicts the inhibition percentage obtained for each incubation time. A time of 5 min displayed the higher inhibition value, so this was chosen as ideal AChE-tacrine incubation time. For this study, N-GQD 1:25 dilution, 27.4 $U \cdot mL^{-1}$ AChE, 14.16 mM ATC and 20 µM tacrine were used.

3.4 Analytical features

The proposed methodology was investigated in terms of analytical efficiency, in order to evaluate its usefulness for quantitative analysis of tacrine in aqueous solutions. As aforementioned, N-GQD fluorescence was no quenched in presence of single AChE or ATC, but the fluorescence attenuation was produced by the enzymatic reaction products. In the presence of tacrine, acting as inhibitor of the AChE activity, the quenched fluorescence of the N-GQDs was progressively restored because of the decrease in product formation. The fluorescence response of N-GQDs to increasing concentrations of tacrine was tested under optimized conditions. The fluorescence intensity of the N-GQDs/AChE/ATC mixture increased with the tacrine concentration.

View Article Online
DOI: 10.1039/C6AN00357E

The inhibition efficiency was used as analytical signal and it was plotted against tacrine concentration for standard solutions. The inhibition efficiency was calculated as follows:

$$Inhibition\ efficiency\ (\%) = \frac{F_{inhibitor} - F_{no\ inhibitor}}{F_0 - F_{no\ inhibitor}} * 100 \quad (27)$$

in which $F_{inhibitor}$ was the fluorescence intensity recorded for the N-GQDs/AChE/ATC mixture in the presence of different inhibitor concentrations; $F_{no\ inhibitor}$ referred to the fluorescence of the same system but in the absence of tacrine, and F_0 to the fluorescence of the N-GQDs/ATC mixture but in the absence of both AChE and tacrine. The inhibition percentage was linearly related to the tacrine concentration between 4-20 μM. Each concentration level was analyzed in triplicate. Error bars depict the standard deviation of the mean value. The equation of the calibration graph was $y=3.1698x+0.9008$ ($R^2=0.994$). Figure 6 shows the fluorescence spectra obtained for different tacrine concentrations. As can be observed, the N-GQD fluorescence is quenched when the enzymatic reaction takes place (AChE+ATC). However, increasing concentrations of tacrine in the system led to a greater recovered fluorescence signal. The inset of the figure illustrates the calibration curve of the proposed sensing method.

The theoretical limits of detection (LOD) and quantification (LOQ) were calculated as 3Sa/b and 10Sa/b, respectively, Sa being the standard error of the intercept and b the slope of de calibration curve (n = 3). The values found were a LOD and a LOQ of 1.22 μM and 4.05 μM, respectively. The precision, expressed as relative standard deviation (RSD) in terms of repeatability (n = 7), was 4.85% at a concentration level of 7 μM.

<<Figure 6>>

View Article Online
DOI: 10.1039/C6AN00357E

3.5 Real samples measurements

The optimized method was finally validated in river water samples. Direct analyses on river water did not provide good results, what it was attributed to the presence of effectors of AChE in the matrix. These effectors led to the overestimation of the tacrine content in real samples and for this reason, an additional preconditioning step was included for reducing interferences. River water samples was spiked with inhibitor and then filtered through solid-phase extraction (SPE) cartridges containing SAX as sorbent phase at a flow rate of 1 $mL \cdot min^{-1}$. Several assays were firstly conducted in order to confirm that tacrine was not retained also in the SPE cartridges along with other interferences. For this purpose, samples were spiked before and after of filtration at the same concentration, and the analytical signals were compared. Results corroborated the absence of retention of tacrine in the SAX sorbent. Prior to filtration of river water samples through cartridges, these were preconditioned following the manufacturer´s instructions, that is, with 1 mL of ultrapure water, 1 mL of 0.1 M ammonium acetate and 1 mL of 15 mM ammonium acetate. Afterwards, the treated river water samples were analyzed by the optimized sensing method. By comparison with standards in ultrapure water, recoveries were in the range 80-92% with reproducibility values, in terms of %RSD, of 3.81% (n=3).

4. Conclusions

In this study, a novel optical sensor based on fluorescent N-GQDs and enzymatic inhibition mechanisms has been developed. Nanoparticles resulted to be sensitive to the AChE activity, since a quenching effect on fluorescence signal was observed only in presence of enzymatic reaction products. The inclusion of tacrine, inhibitor of AChE,

View Article Online
DOI: 10.1039/C6AN00357E

reduced the activity of enzyme to convert substrate into products, and consequently, the N-GQD fluorescence was progressively recovered by increasing the tacrine concentration in the assay solution. Experimental results showed an excellent linear relationship between the analytical signal (percent inhibition efficiency) and tacrine concentration in the range of 4-20 μM (R^2=0.994). While our sensor is characterized by simplicity (consecutive addition of species into assay solution), rapidity (≈15 min of analysis) and good reprodubility (RSD<5%), the limit of detection for tacrine determination was found to be in the micromolar range, resulting certainly superior to some reported in literature for other biosensing approaches.[28-31] Most of them use gold/silver nanoparticles/nanoclusters as fluorescent probes and include several bioconjugation steps for performing the sensing mechanism. However, the sensitivity of our proposed GQD-based sensor is in accordance with other fluorescence bioassays involving the use of carbon quantum dots.[32] In addition, we here propose a promising analytical strategy without any requirement of immobilization step (i.e. bioconjugation between nanoparticle and enzyme) or the presence of other intermediary species in solution, such as Cu^{2+}, what finally simplifies and hastens our method in comparison with others already described. The presented methodology could be compatible with the use of other esterase family members such as Butyrylchoinesterase (BChE) and Carboxylesterase (CaE) which their interaction with tacrine has been recently described.[33]

Acknowledgements

The authors want to thank to the Ministry of Economy and Competitiveness for financial support (project CTQ2014-52939R).

View Article Online
DOI: 10.1039/C6AN00357E

The authors have declared no conflict of interest.

View Article Online
DOI: 10.1039/C6AN00357E

References

1 S. Carregal-Romero, E. Caballero-Díaz, A.M. Abdelmonem, D. Hühn, M. Valcárcel, L. Beqa, M. Ochs, B.S. Suau and W.J. Parak, *Annu. Rev. Anal. Chem.*, **2013**, 6, 53.

2 J.E. Morris and K. Iniewski, *Graphene, Carbon Nanotubes, and Nanostructures: Techniques and Applications*. CRC Press, Florida, 2013.

3 S. Benítez-Martínez and M. Valcárcel, *TrAC-Trends*, **2015**, 72, 93-113.

4 L. Zhou, J. Geng and B. Liu, *Part. Part. Syst. Charact*, **2013**, 30, 1086-1092.

5 X. Liu, W. Gao, X. Zhou and Y. Ma, *J. Mater. Res.*, **2014**, 29, 1401-1407.

6 L. Zhang, Z. Zhang, R. Liang, Y. Li and J. Qiu, *Anal. Chem.*, **2014**, 86, 4423-4430.

7 Z. Wu, W. Li, J. Chen and C. Yu, *Talanta*, **2014**, 119, 538-43.

8 J. Liu, X. Zhang, Z. Cong, Z. Chen, H. Yang and G. Chen, *Nanoscale*, **2013**, 5, 1810-1815.

9 T.V. Tam, N.B. Trung, H.R. Kim, J.S. Chung and W.M. Choi, *Sens. Actuat. B,* **2014**, 202, 568-573.

10 S. Li, Y. Li, J. Cao, J. Zhu, L. Fan and X. Li, *Anal. Chem.*, **2014**, 86, 10201-10207.

11 B. Zhang, H. Gao and X. Li, *New J. Chem.*, **2014**, 38, 4615-4621.

12 P. Kumar, K.-H. Kim and A. Deep, *Biosens. Bioelectron.*, **2015**, 70, 469-481.

13 M. Saleem, L.P. Leeb and K.H. Lee, *J. Mater. Chem. B*, **2014**, 2, 6802-6808.

14 F. Mao, J. Li, H. Wei, L. Huang and X. Li, *J. Enzyme Inhib. Med. Chem.*, **2015**, 30, 995-1001.

15 D.N. Kumar, S.A. Alex, R.S.S. Kumar, N. Chandrasekaran and A. Mukherjee, *Colloid. Surface. A*, **2015**, 485, 111-117.

View Article Online
DOI: 10.1039/C6AN00357E

16 A.R. Mukhametshina, S.V. Fedorenko, I.V. Zueva, K.A. Petrov, P. Masson, I.R. Nizameev, A.R. Mustafina and O.G. Sinyashin, *Biosens. Bioelectron.*, **2016**, 77, 871-878.

17 R.M, Kestwal, D. Bagal-Kestwal and B.-H. Chiang, *Analytica Chim. Acta*, **2015**, 886, 143-150.

18 N. Chauhan and C.S. Pundir, *Analytica Chim. Acta*, **2011**, 701, 66–74.

19 L. Zhang, L. Long, W. Zhang, D. Du and Y. Lin, *Electroanal.*, **2012**, 24,1745-1750.

20 H. Zhao, X. Ji, B. Wang, N Wang, X. Li, R. Ni and J. Ren, *Biosens. Bioelectron.*, **2015**, 65, 23-30.

21 A. Minarini, A. Milelli, E. Simoni, M. Rosini, M.L. Bolognesi, C. Marchetti and V. Tumiatti, *Curr. Top. Med. Chem.*, **2013**, 13, 1771-1786.

22 S. Benítez-Martínez and M. Valcárcel, *Anal. Chim. Acta*, **2015**, 896, 78-84.

23 V. Tumiatti, A. Minarini, M.L. Bolognesi, A. Milelli, M. Rosini and C. Melchiorre, *Curr. Med. Chem.*, **2010**, 17, 1825-1838.

24 M. Pohanka, *Analytical Letters*, **2013**, 46, 1849-1868.

25 S. Benítez-Martínez and M. Valcárcel, *Sens. Actuat. B*, **2014**, 197, 350-357.

26 B. Shi, L. Zhang, C. Lan, J. Zhao and S. Zhao, *Talanta*, **2015**, 142, 131-139.

27 Q. Long, H. Li, Y. Zhang and S. Yao, *Biosens. Bioelectron.*, **2015**, 68, 168-174.

28 Y. Zhang, T. Hei, Y. Cai, Q. Gao and Q. Zhang, *Anal. Chem.*, **2012**, 84, 2830-2836.

View Article Online
DOI: 10.1039/C6AN00357E

29 W. Li, W. Li, Y. Hu, Y. Xia, Q. Shen, Z. Nie, Y. Huang and S. Yao, *Biosens. Bioelectron.*, **2013**, 47, 345-349.

30 M. Pohanka and V. Vlcek, *Interdiscip. Toxicol.,* **2014**, 4, 215-218.

31 J. Sun and X. Yang, *Biosens. Bioelectron.,* **2015**, 74, 177-182.

32 Z. Qian, L. Chai, C. Tang, Y. Huang, J. Chen and H. Feng, *Sens. Actuat. B,* **2016**, 222, 879-886.

33 G.F. Makhaeva, S.V. Lushchekina, O.G. Serebryakova, T.S. Stupina, A.A. Terentiev, I.V. Serkov, A.N. Proshin, S.O. Bachurin and R.J. Richardson, *Bioorgan. Med. Chem.*, **2016**, 24, 1050-1062.

View Article Online
DOI: 10.1039/C6AN00357E

FIGURE CAPTIONS

Figure 1. HR-TEM image and FT-IR spectrum of N-GQDs.

Figure 2. Scheme illustrating the principle of GQD-based biosensor.

Figure 3. Fluorescence spectra of N-GQDs+ATC (8.09 mM) and N-GQDs+ATC (8.09 mM)+AChE (13.7 $U \cdot mL^{-1}$). λ_{ex}= 355 nm and λ_{em}= 440 nm. Slit width for excitation and emission was adjusted at 2 nm.

Figure 4. Quenching effect on the fluorescence of N-GQDs by testing different concentrations of AChE (0-27.4 $U \cdot mL^{-1}$). Experimental conditions: ATC (8.09 mM) and N-GQDs (1:10 dilution). I_O and I correspond to the fluorescence intensity of N-GQDs in the absence and presence of AChE, respectively. λ_{ex}= 355 nm and λ_{em}= 440 nm. Slit width for excitation and emission was adjusted at 2 nm. Values represent the mean and standard deviation obtained from three separate experiments for each concentration level.

Figure 5. Influence of the N-GQD dilution in the fluorescence quenching response. Experimental conditions: AChE (27.4 $U \cdot mL^{-1}$), ATC (14.16 mM). I_0 and I correspond to the fluorescence intensity of N-GQDs+ATC and N-GQDs+ATC+AChE, respectively. λ_{ex}= 355 nm and λ_{em}= 440 nm. Slit width for excitation and emission was adjusted at 2 nm. Values represent the mean and standard deviation obtained from three separate experiments for each dilution.

Figure 6. Fluorescence spectra and calibration curve of N-GQD-AChE system, under optimal experimental conditions, in presence of various concentrations of tacrine inhibitor (0-20 μM). λ_{ex}= 355 nm and λ_{em}= 440 nm. Slit width for excitation and emission was adjusted at 3.5 nm. Calibration curve data, expressed as inhibition

View Article Online
DOI: 10.1039/C6AN00357E

efficiency (%), represent the mean and standard deviation obtained from three separate experiments for each level of concentration.

View Article Online
DOI: 10.1039/C6AN00357E

FIGURES

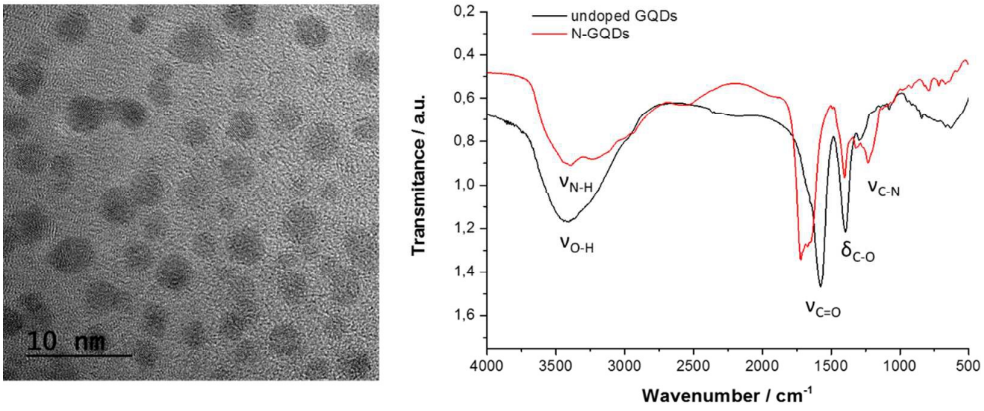

New Figure 1

View Article Online
DOI: 10.1039/C6AN00357E

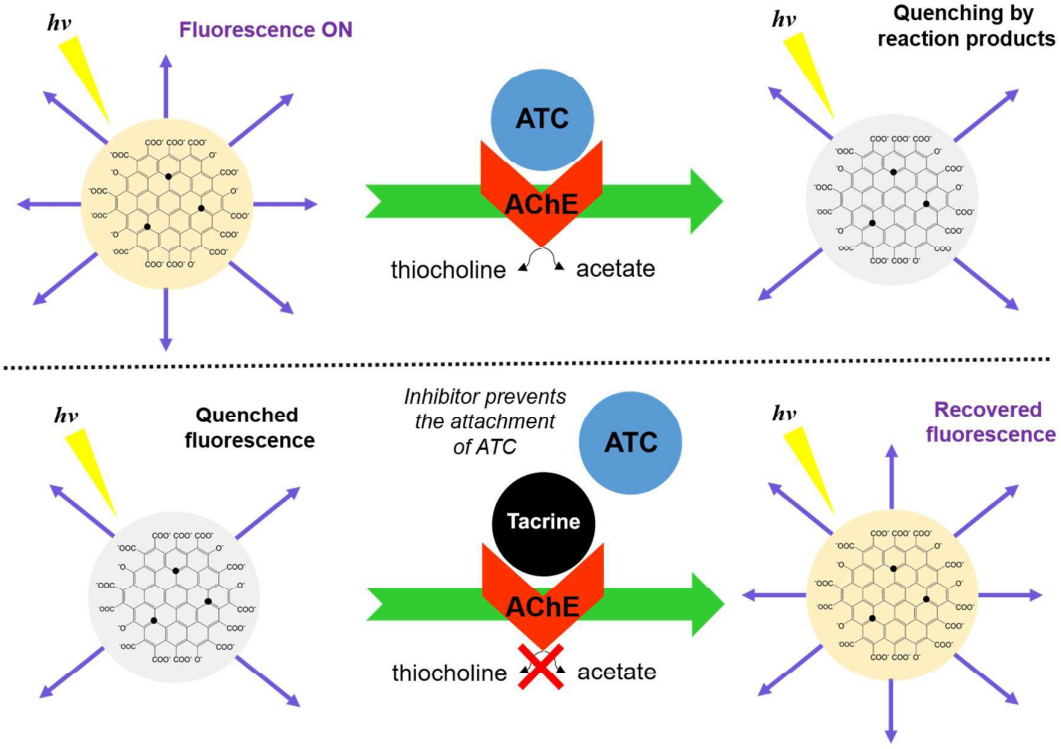

Figure 2

View Article Online
DOI: 10.1039/C6AN00357E

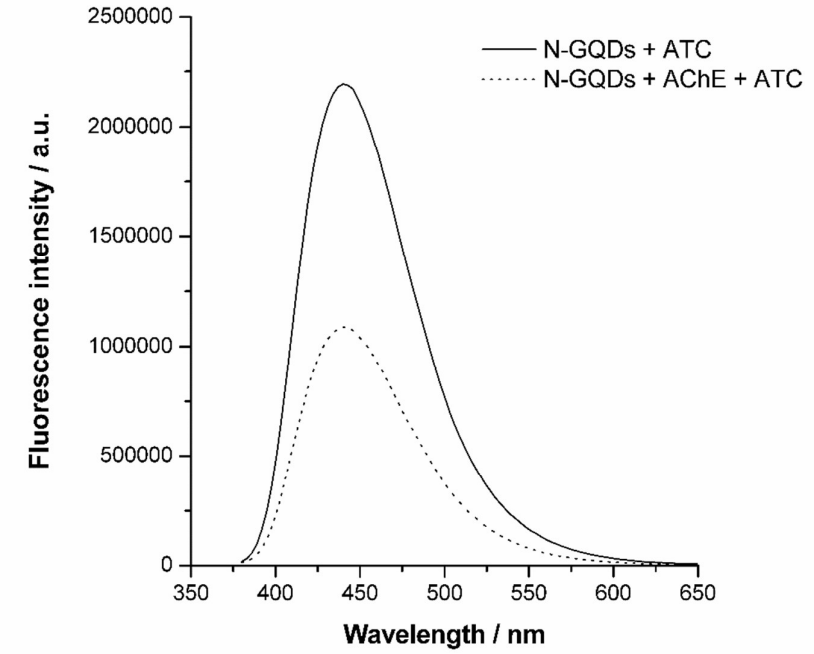

New Figure 3

View Article Online
DOI: 10.1039/C6AN00357E

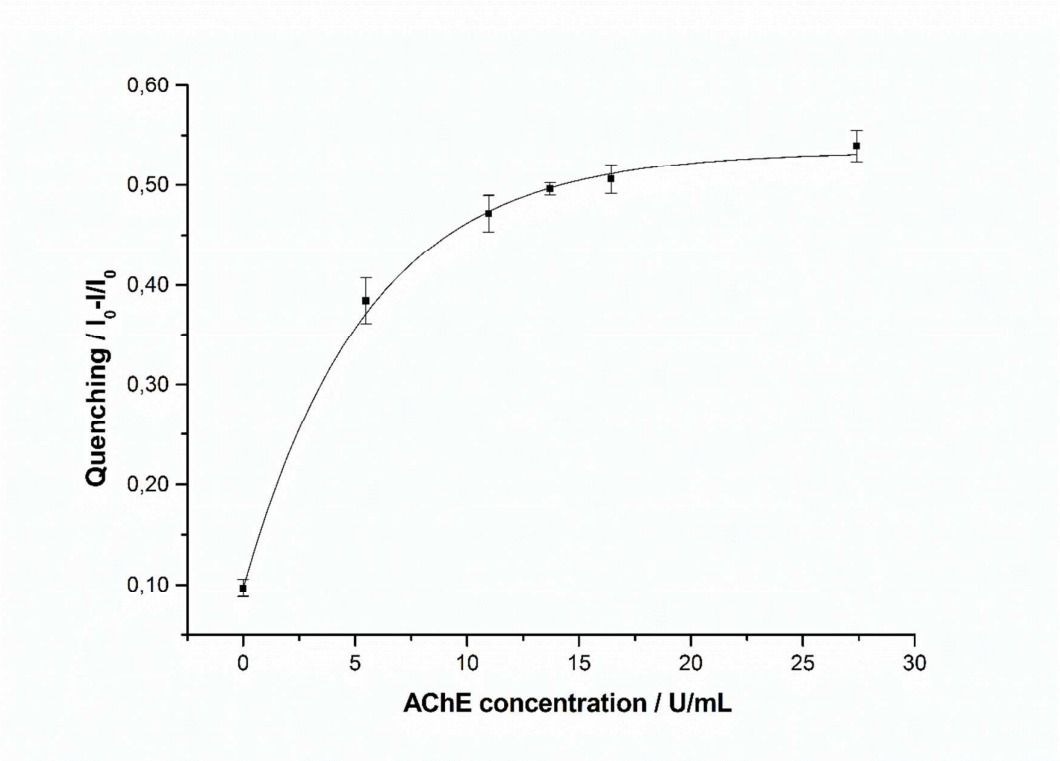

Figure 4

View Article Online
DOI: 10.1039/C6AN00357E

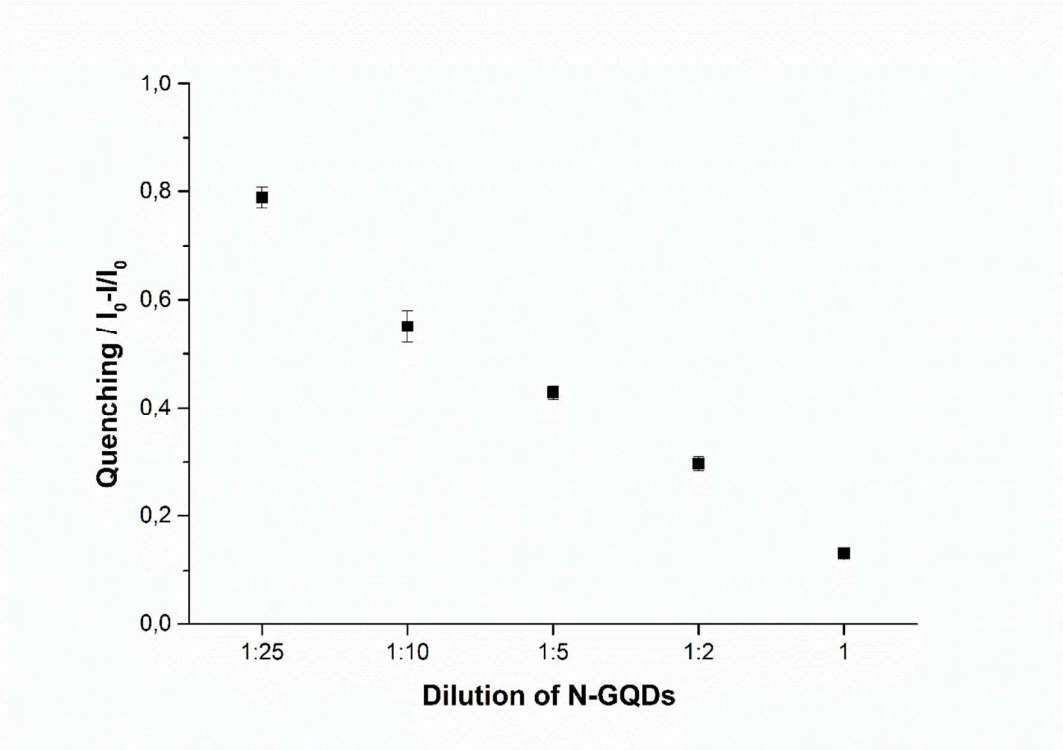

Figure 5

View Article Online
DOI: 10.1039/C6AN00357E

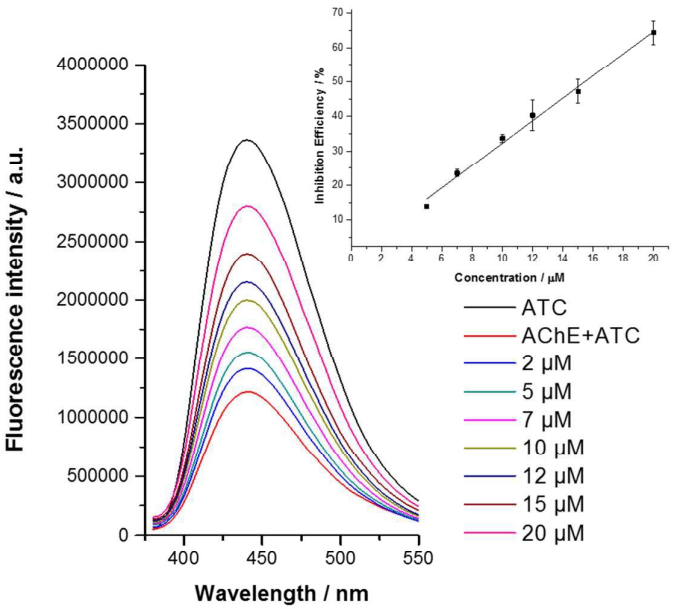

Figure 6

View Article Online
DOI: 10.1039/C6AN00357E

For TOC only:

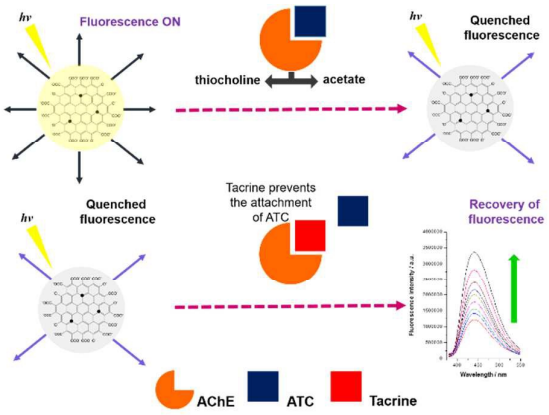

The graphene quantum dot-based sensor is sensitive to reaction products resulting from acetylcholinesterase activity and it allows for determination of tacrine acting as enzyme inhibitor.